



Norwegian University of
Science and Technology

Pressure measurements inside a Francis turbine runner

Einar Agnalt

Master of Science in Mechanical Engineering

Submission date: June 2016

Supervisor: Ole Gunnar Dahlhaug, EPT

Co-supervisor: Torbjørn Nielsen, EPT

Pål-Tore Storli, EPT

Carl Bergan, EPT

Norwegian University of Science and Technology

Department of Energy and Process Engineering



Norwegian University
of Science and Technology

Department of Energy
and Process Engineering

EPT-M-2016-05

MASTER THESIS

for

Einar Agnalt

Spring 2016

Pressure measurement inside a Francis turbine runner

Trykkmålinger inne i et Francis løpehjul

Background

The average age of Norwegian hydro power plants are 45 year, and many show sign of fatigue and needs to be constantly maintained or refurbished. Additionally, some power plants in Norway has experienced failures on new Francis runners: Driva-, Sønnå-, Svartisen-, Hol 1-, Eriksdal-, Brokke- and Vinje Power Plant. The main problem is the formation of cracks in the turbine runner.

The main challenges for the numerical analysis of the Fluid-Structure Interaction (FSI) on high head Francis turbines originates in the natural frequency of the turbine runner and the fluid properties of the existing pressure oscillations.

Recently, researchers in the Waterpower Laboratory at the Norwegian University of Science and Technology, (NTNU) designed their own High head Francis turbine and published both geometry and model performance data in order to provide other researchers with a relevant case to work with and to promote the Francis-99 workshops. The Francis-99 workshops aim to determine the state of the art of high head Francis turbine simulations (flow and structure) under steady and transient operating conditions as well as promote their development and knowledge dissemination openly. This project will provide some of the necessary measurements needed for the Francis-99 workshops and knowledge to understand how to carry out measurements of the stresses on the turbine runner blades. The work will be in close cooperation with Katarina Kloster.

Objective

Measurement of pressure inside a Francis turbine runner.

The following tasks are to be considered:

1. Literature study
 - a. Fatigue loads in high head Francis turbines
2. Software knowledge
 - a. Labview
 - b. Creo
3. Laboratory preparations
 - a. Make a complete 3D-drawing of the Tokke model geometry
 - b. Install and calibrate the pressure sensors in the turbine runner.
4. Pressure pulsation measurements based on sensors installed in the draft tube cone, vanless space and in the runner.
5. If an FSI-analysis is available, the measurements will be compared to these.

-- " --

Within 14 days of receiving the written text on the master thesis, the candidate shall submit a research plan for his project to the department.

When the thesis is evaluated, emphasis is put on processing of the results, and that they are presented in tabular and/or graphic form in a clear manner, and that they are analyzed carefully.

The thesis should be formulated as a research report with summary both in English and Norwegian, conclusion, literature references, table of contents etc. During the preparation of the text, the candidate should make an effort to produce a well-structured and easily readable report. In order to ease the evaluation of the thesis, it is important that the cross-references are correct. In the making of the report, strong emphasis should be placed on both a thorough discussion of the results and an orderly presentation.

The candidate is requested to initiate and keep close contact with his/her academic supervisor(s) throughout the working period. The candidate must follow the rules and regulations of NTNU as well as passive directions given by the Department of Energy and Process Engineering.

Risk assessment of the candidate's work shall be carried out according to the department's procedures. The risk assessment must be documented and included as part of the final report. Events related to the candidate's work adversely affecting the health, safety or security, must be documented and included as part of the final report. If the documentation on risk assessment represents a large number of pages, the full version is to be submitted electronically to the supervisor and an excerpt is included in the report.

Pursuant to "Regulations concerning the supplementary provisions to the technology study program/Master of Science" at NTNU §20, the Department reserves the permission to utilize all the results and data for teaching and research purposes as well as in future publications.

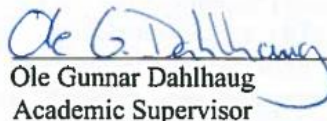
The final report is to be submitted digitally in DAIM. An executive summary of the thesis including title, student's name, supervisor's name, year, department name, and NTNU's logo and name, shall be submitted to the department as a separate pdf file. Based on an agreement with the supervisor, the final report and other material and documents may be given to the supervisor in digital format.

- Work to be done in lab (Waterpower lab, Fluids engineering lab, Thermal engineering lab)
 Field work

Department of Energy and Process Engineering, 11th January 2016



Olav Bolland
Department Head



Ole Gunnar Dahlhaug
Academic Supervisor

Co-Supervisors:

- Torbjørn K. Nielsen
- Pål-Tore S. Storli
- Carl Bergan

PREFACE

This master thesis has been written at the Waterpower Laboratory, Department of Energy and Process Engineering at the Norwegian University of Science and Technology during the spring 2016.

This thesis has been written and formulated as a scientific paper. The intention is to try to publish the article, which is a little scary, but a great inspiration. The work has been in cooperation with Katarina Kloster and her monolog presents measurements from the same laboratory experiment. I would like to thank Katarina for the great partnership during this semester. Without all our discussions, the results would not have been the same.

In addition, a great thank you to my supervisor Ole Gunnar Dahlhaug for letting me plan and accomplish these measurements the last year. Without you believing in the project, the progress would not been the same. Another great thank you to Carl Bergan for your exceptional help with all the challenges in the experiment.

Finally, I would like to thank my friends and wife for letting me spend our valuable time working with this project.



Einar Agnalt

This page has intentionally been left blank

ABSTRACT

Over the last years, there have been several incidents with cracks in high head Francis turbines. These cracks are understood to be related to pressure pulsations, vibration modulus and combination of these. In this paper, an investigation of pressure pulsations in a High Head model turbine is performed with the use of onboard pressure sensors and strain gauge. Earlier onboard measurements have mainly utilized blade-mounted sensors. In this paper, a setup with hub-mounted pressure sensors are described. In addition, a strain gauge mounted on the trailing edge of one blade is used to relate the measured pressure to the loading on the blade. Results from the measurements gave a good but not complete picture of the wave propagation through the runner. The most dominating frequency was the guide vane passing frequency on both the pressure measurements and the strain measurements. The measurements did not provide all necessary information for full analysis of the onboard pressure pulsations. On the other hand, the setup is considered as a good reference for computational fluid dynamics validation (CFD) and is considered less extensive for evaluating the onboard pressure pulsations compared to blade-mounted sensors.

SAMMENDRAG

I løpet av de siste årene har det vært flere hendelser med sprekker i høytrykks francisturbiner. Disse sprekker er forstått å være relatert til trykkpulsasjoner, vibrasjonsmodulus og kombinasjoner av disse. I denne artikkelen, er en undersøkelse av trykkpulsasjoner i en høytrykks Francis modellturbin utført ved bruk av trykksensorer og strekklapp montert i løpehjulet. Tidligere tilsvarende målinger har i hovedsak benyttet bladmonterte sensorer. I denne utredningen, er et oppsett med sensorer montert bosset beskrevet. I tillegg er det montert en strekklapp på bakre kant av et blad for å relatere trykkmålinger til bevegelse av bladet. Resultatene fra målingene ga et godt bilde av bølgeforplantning gjennom løpehjulet, men ikke helt komplett. Den mest dominerende frekvens var ledskovelpassering både på trykkmålinger og strekkmålinger. Målingene gav ikke alle svar på bølgefysikken inni hjulet, men er ansett som en god referanse for sammenligning med Computational Fluid Dynamics (CFD). I tillegg er oppsettet regnes som mindre omfattende i forhold til bladmonterte sensorer.

Analysis of onboard pressure pulsations and its influence on blade loading in a High Head Francis model turbine.

Einar Agnalt, Ole Gunnar Dahlhaug

ainer.agnalt@ntnu.no

Norwegian University of Science and Technology
Department of Energy and Process Engineering

Abstract— Over the last years, there have been several incidents with cracks in high head Francis turbines. These cracks are understood to be related to pressure pulsations, vibration modulus and combination of these. In this paper, an investigation of pressure pulsations in a High Head model turbine is performed with the use of onboard pressure sensors and strain gauge. Earlier onboard measurements have mainly utilized blade-mounted sensors. In this paper, a setup with hub-mounted pressure sensors are described. In addition, a strain gauge mounted on the trailing edge of one blade is used to relate the measured pressure to the loading on the blade. Results from the measurements gave a good but not complete picture of the wave propagation through the runner. The most dominating frequency was the guide vane passing frequency on both the pressure measurements and the strain measurements. The measurements did not provide all necessary information for full analysis of the onboard pressure pulsations. On the other hand, the setup is considered as a good reference for computational fluid dynamics validation (CFD) and is considered less extensive for evaluating the onboard pressure pulsations compared to blade-mounted sensors.

Index Terms— Onboard pressure pulsations; high head Francis Turbine

Nomenclature

Symbol	Description	Unit
Friction factor and basic equation:		
Z_g	Number of guide vanes	[—]
Z_b	Number of runner blades	[—]
f_0	Runner frequency	[s^{-1}]
f_g	Guide vane passing frequency	[s^{-1}]
f_b	Blade passing frequency	[s^{-1}]
m	Harmonic number	[—]
ϕ	Phase angle	[rad]
P	Pressure	[Pa]
R	Reflection coefficient	[—]
g	Guide vane	[—]
b	Blade	[—]
RSI		

I. INTRODUCTION

The high focus on environment and green energy together with aging Norwegian Hydropower leads to refurbishment of power plants and new turbines. Some new power plants with installed Francis runner have experienced breakdown after few running hours. The design and calculations of runners are based on numerical analysis, but the main problem is to get reliable results regarding fluid structure interaction in the runner. The biggest issue is crack propagation and its origin. For a better understanding of the physics behind this problem, model testing and computer simulations must be performed. Pressure pulsations and vibrations lead to cyclic stress on the turbines and potential fatigue damage. Furthermore, a high focus on savings related to materials leads to more vulnerability to fatigue cracks[1].

In high head hydropower (HPP) with Francis turbines, the rotor stator interaction (RSI) is the most dominating frequency[2]. Several studies focuses on this interaction and the possible interference between the travelling waves around the runner[3]–[5]. The wave created by the runner blades passing the guide vanes are mainly found outside the runner between upper and lower cover, through the guide vane section and in the spiral casing. Measurements on prototypes revealed high amplitudes with the blade passing frequency due to a certain combination of blade numbers and guide vane numbers[3], [4].

When considering the waves inside a HPP Francis runner, the main frequencies found on strain gauge measurements are related to RSI and its harmonics. In addition, studies with onboard measurements shows that other frequencies are present as well. At part-load, the helical vortex rope induces pressure fluctuations with both an asynchronous and a non-rotation synchronous component. It is shown that only the asynchronous has impact on the blade loading [6]. The main method found for onboard measurements, are with the use of blade-mounted sensors. One experiment with this setup concluded with good results[7]. This is also done on the same runner as current measurement, but the complexity of the setup and durability of

the sensors was not satisfactory[8]. In this paper, a measurement method with hub mounted pressure sensors and blade mounted strain gauge, is used to analyze the influence on trailing edge loading from rotor stator interaction onboard a high Francis model runner. The setup utilizes a high sampling rate to be able to analyze the details of the waves on both sides of a blade and the correlation to strain.

A. Theory

In HPP with installed Francis runners, the frequencies with predominant amplitudes are related to rotor stator interaction RSI, guide vane frequency and blade passing frequency[9]. This phenomenon is well described as by Tanaka[10]. The pressure waves from the guide vane passing is mainly found in the runner channels while the blade passing frequency is mainly found in the vaneless space between the runner and guide vane cascade and propagating into the spiral casing[4]. The frequencies and its harmonics are from the relationship between number of blades and number of guide vanes. Kubota et.al [11] used the connection to diameter mode and Rodriguez et.al [12] further connected this to the sequence of interaction, when and where the passing occurs. In this paper the notation RSI_g^m and RSI_b^m will be used for guide vane frequency and blade passing frequency respectively. The harmonic number is m .

The relative phase shift of the RSI frequencies is from a geometric point of view:

$$\phi_{RSI}^m = m \cdot 2 \cdot \pi \cdot \left(\frac{Z_g}{Z_b} - 1 \right) [rad] \quad (1)$$

The phase shift is for two neighboring channels, thus channels with more than one blade between will have an increased shift as a multiple of single blade shift.

Two neighboring channels will have a pressure difference due to phase shift:

$$\Delta P^m = 2 \cdot \sin(\phi_{RSI}^m + \pi) [-] \quad (2)$$

A phase difference of -0.5π gives double pressure difference illustrated in figure. P1 and P2 are pressures on each side of a blade.

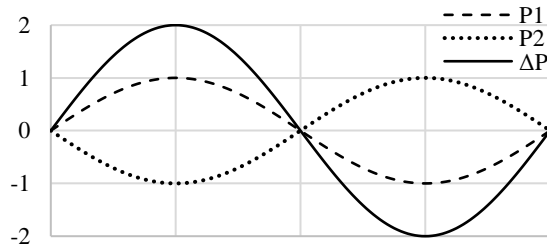


Figure 1 Differential pressure with $-0.5 \cdot \pi$ phase shift.

The time delay of the phase shift is related to the runner frequency f_0 and is equal for all harmonics:

$$RSI_{\Delta t}^{b,g} = \frac{\phi_{RSI}}{m \cdot 2 \cdot \pi \cdot f_0 \cdot Z_{b,g}} \quad (3)$$

When considering a travelling wave through a channel, any discontinuity in the properties of the channel, can cause the wave front to be reflected. Discontinuities are changes in area, changes in the elasticity of the walls, division into branches and more. The amount of reflected energy and the reflected phase are described with a reflection coefficient R . For a closed end pipe, the coefficient is $R = 1$ which means total reflection with no phase shift. With an open-ended pipe or into a reservoir $R = -1$ which is total reflection with 180 degree phase shift. The pressure pulse in a travelling wave will move with the speed of sound. When reflection occurs, the combination of forward and reflected wave results in a standing wave. These waves gives a situation where there is no energy transmission in the system. In any viscous system with oscillatory motion, there will be losses, thus there will always be a travelling wave since the reflected wave has less energy[13].

II. EXPERIMENTAL SETUP

The experiment was done in the Waterpower Laboratory at Norwegian University of Science and Technology, NTNU. Figure 2 gives an overview of the Francis test rig setup. The runner is a splitter design with 15+15 blades. The number of guide vanes is 28. Several recent measurements are available with this model related to the Francis-99 project, both steady state and transient operations [14].

The predominant frequencies in the NTNU Francis test rig are summarized in Table 1

Frequency	$[s^{-1}]$
Guide vane passing f_g	$28f_0$
Blade passing f_b	$30f_0$
Rheinegans f_r	$\sim 0,3f_0$
Upstream standing wave	~ 15
Downstream standing wave	~ 42
Known noise frequencies	
Generator control	300 and 600

Table 1 Known frequencies in NTNU test rig

The strain gauges mounted on the blade are semiconductor-based because of high sensibility compared to metal foil gauges. The data acquisition was done through a slip-ring, enabling full synchronization between rotating and stationary domain. Custom-built amplifiers mounted on the shaft did the conversion from bridge output to $\pm 10V$ and in this way increased the signal to noise ratio through the slip-ring system.

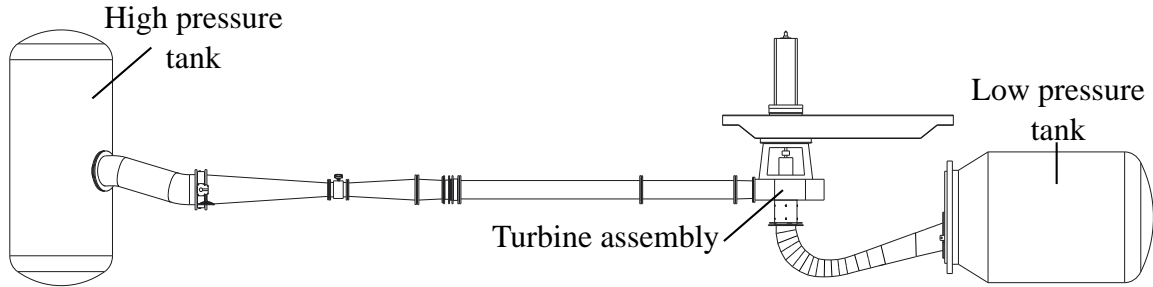


Figure 2 Overview of measurement setup

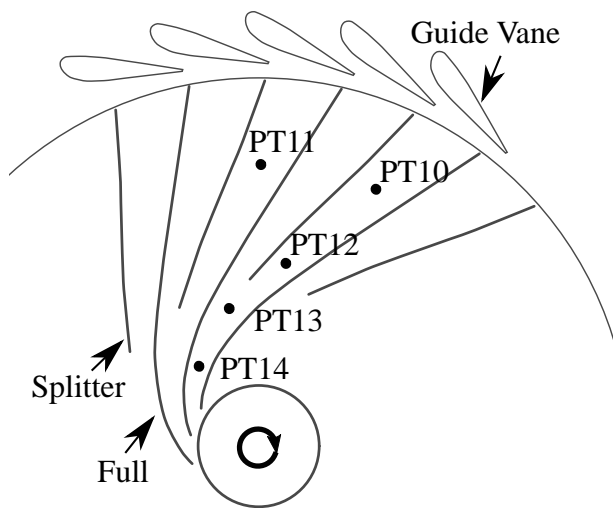


Figure 3 Position of pressure sensors over runner channels.

The pressure sensors were Kulite XTE-190(m) with range from 0-3,5bara. Five sensors were flush mounted in the hub as seen in **Figure 3** and **Figure 4**. Two sensors in separate channels at the inlet (PT10-PT11), upstream splitter (PT12), downstream splitter (PT13) and one close to the outlet (PT14). The distance between the sensors are summarized in Table 2

PT10 to PT12	$104,6 \pm 0,1$
PT12 to PT13	$69,6 \pm 0,1$
PT13 to PT14	$61,6 \pm 0,1$

Table 2 Distance between sensors [mm]

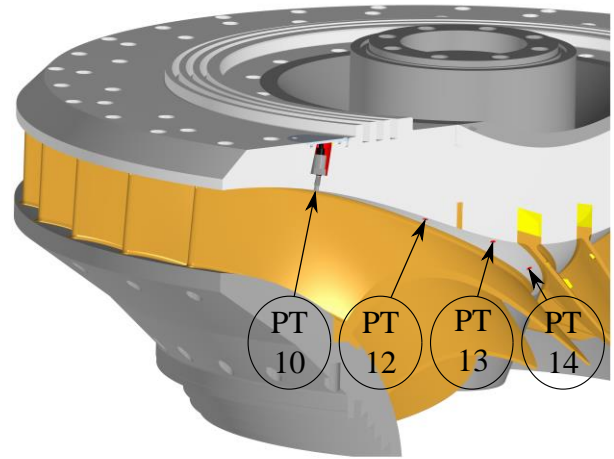


Figure 4 PT10, PT12, PT13 and PT14 mounted in the hub.

The strain gauge was Kulite S/UDP-350-175 in quarter Wheatstone bridge configuration. This configuration makes no temperature compensation. A zero point reference was taken before and after experiment. This indicated a zero point drift, hence the stationary values are considered invalid. However, the frequencies and the ratio between amplitudes can give a good indication of the connection between pressure pulsations and blade movement. A single strain gauge will not be sufficient for determination of blade loading since the output is one directional strain.

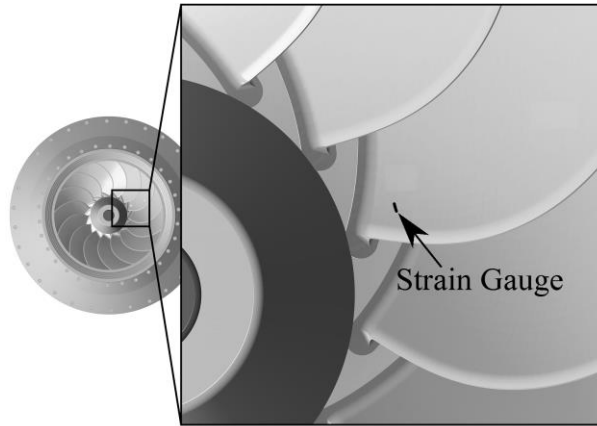


Figure 5 Strain gauge on blade.



Figure 6 Picture of strain gauge on blade.

Data acquisition (DAQ) was done with Labview and cDAQ from National Instruments. Maximum sample speed with available equipment was $50k [Hz]$. All DAQ inputs were equipped with elliptic anti-aliasing filter. All wires were shielded and connected to a common reference. The complete setup is illustrated in **Figure 7**

A. Calibration and setup verification

Pressure sensors were calibrated with a dead weight manometer with air as medium. This was done without rotation of the slip-ring. Total uncertainty for the pressure measurements includes uncertainty of calibration method and regression line from calibration. The uncertainty was found to be $\max \pm 0,2\%$ in the operating range. Because the slip ring will rotate during measurements, a comparison of noise with and without rotation was carried out with a constant $10V$ signal from a precision voltage source mounted on the shaft. The noise floor was found to be $6\mu [V_{rms}]$, which is below the technical noise floor of the voltage supply, and thus the noise addition through the slip-ring is negligible in this experiment. The measurements are dynamic and the amplitude reduction is documented to not be more than $-3dB$ for frequencies up to $25k [Hz]$. The measured amplitudes below this frequency are therefore considered to be within the steady calibrated uncertainty.

The strain gauge was not calibrated, but the relative uncertainty of the theoretical output from the amplifier was calculated with root-sum-squares as described by Kalita

et.al[15]. The uncertainty was found to be $\max \pm 0,25\%$ in the operating range.

B. Post processing

To evaluate frequencies, FFT was used with Welch's method. To evaluate phase between signals, mean and 95% confidence interval was calculated from multiple FFT with different signal lengths. To verify the FFT, inverse FFT was calculated and compared to original signal. A filtered signal was used together with the raw signal as an additional evaluation method for the amplitudes.

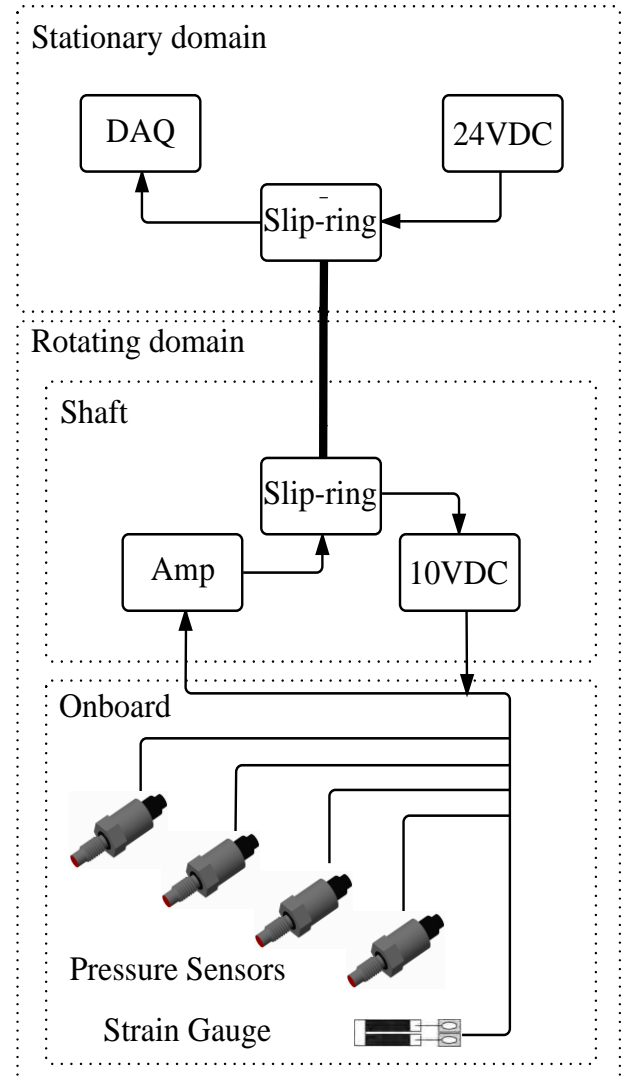


Figure 7 DAQ setup.

C. Operation points

Three operating points were tested. Part load (PL), Best efficiency point (BEP) and High Load (HL) as summarized in Table 3

	PL	BEP	HL
Guide vane angle [deg]	6,9	10,1	12,6
n_{ED} [-]	0,179	0,178	0,177
Q_{ED} [-]	0,106	0,152	0,184

Table 3 Operation points

III. RESULTS

The results are presented from inlet to outlet of the runner. First, the phase shift is evaluated with PT10 and PT11. Further, the amplitudes and timing of the pressure waves inside the runner channel measured by PT10, PT12, P13 and PT14 are presented. Strain is presented as FFT with relative amplitudes. Finally, the differential pressure over one blade trailing edge is calculated for the correlation between the pressure and the strain measurements.

Theoretical RSI phase shift, calculated from equation (1).

$$\phi_{RSI}^1 = -\frac{2}{15} \cdot \pi \approx -0,419 [rad] \quad (4)$$

PT11 and PT10 is placed with two blades between, thus the phase shift will be twice the calculation of two neighboring channels:

$$\phi_{RSI}^1|_{11-10} = \frac{4}{15} \cdot \pi \approx 0,838 [rad] \quad (5)$$

FFT was used to find the phase shift for RSI_g^1 and RSI_g^2 from the measurements. The results are presented in Table 4.

	PL		BEP		HL	
	ϕ_{RSI}	Dev	ϕ_{RSI}	Dev	ϕ_{RSI}	Dev
RSI_g^1	0,841	+0,4	0,838	0	0,838	0
RSI_g^2	1,708	+1,9	1,807	+7,8	2,120	+26,5

Table 4 FFT calculation of phase shift in [rad] from the measurements and deviation from calculations with equation (1) [%].

The measured signal from PT11 and PT10 is presented in **Figure 8**. The dominating frequency is the guide vane frequency. With current runner speed, the signal from PT10 must be moved forward 13,7 ms in time to be measuring the same guide vane passing as PT11.

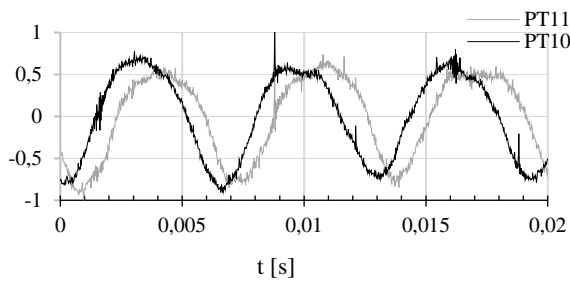


Figure 8 Raw signals from PT10 and PT11 at BEP. Mean is subtracted and amplitudes are normalized to common max.

To identify the different frequencies at the inlet of the runner, a FFT of PT10 is presented in **Figure 9**. The most dominating is $RSI_g^1 = 155 [Hz]$ and $RSI_g^2 = 310 [Hz]$. The blade passing frequency $RSI_b^1 = 166 [Hz]$ is also visible. Other peaks with lower frequencies are related to runner frequency and the rotating vortex rope in the draft tube, but this is not focused on in this paper. For comparison of pressure amplitudes, all peaks are related to RSI_g^1 for normalizing.

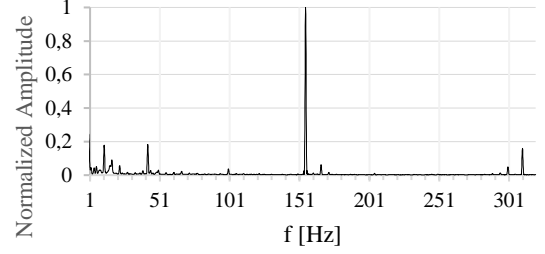


Figure 9 FFT of PT10 normalized amplitudes to max amplitude guide vane passing. Running point is BEP

The average amplitudes through the runner channel is presented for RSI_g^1 in **Figure 10** and for RSI_g^2 in **Figure 11**. The amplitudes are calculated by Welch's method and verified by analysis of raw signal and by filtering the frequency of interest.

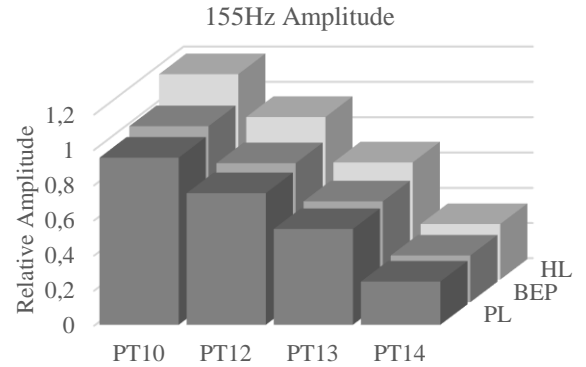


Figure 10 Relative amplitudes of RSI_g^1 on different running points through the runner.

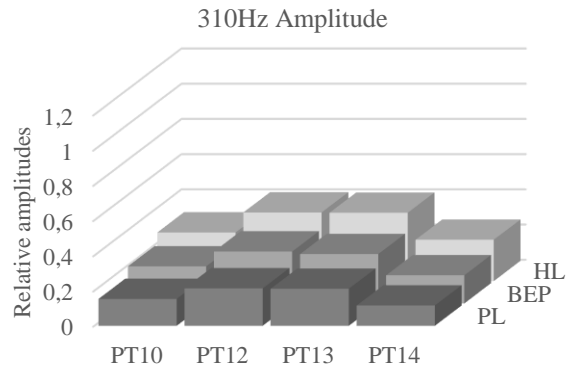


Figure 11 Relative amplitudes of RSI_g^2 on different running points through the runner.

Time delay between the different sensors through the channel is presented in Table 5. The delay is presented with velocity and time calculated from equation (3) based on FFT phase evaluation and distance from Table 2. This was found most convenient because the distances between sensors are not equal, thus by evaluating speed, both time delay and distance is considered.

RSI_g^1	PL		BEP		HL	
	t	v	t	v	t	v
10 to 12	93	891	101	968	106	1016
12 to 13	50	721	53	764	51	730
13 to 14	-20	-333	-7	-116	-15	-249
RSI_g^2	t	v	t	v	t	v
10 to 12	-58	-553	-87	-836	-90	-864
12 to 13	-77	-1104	-81	-1169	-86	-1241
13 to 14	-36	-582	-35	-573	-43	-698

Table 5 Wave speed [m/s] and time [ms] through runner. PT is not included for the pressure sensor number.

Results from the strain gauge is presented in Figure 12. It is clear that the domination frequencies are 42 [Hz], RSI_g^1 and RSI_g^2 . From Table 1, 42 [Hz] is known to be a standing wave downstream the runner and is not included in the current analysis.

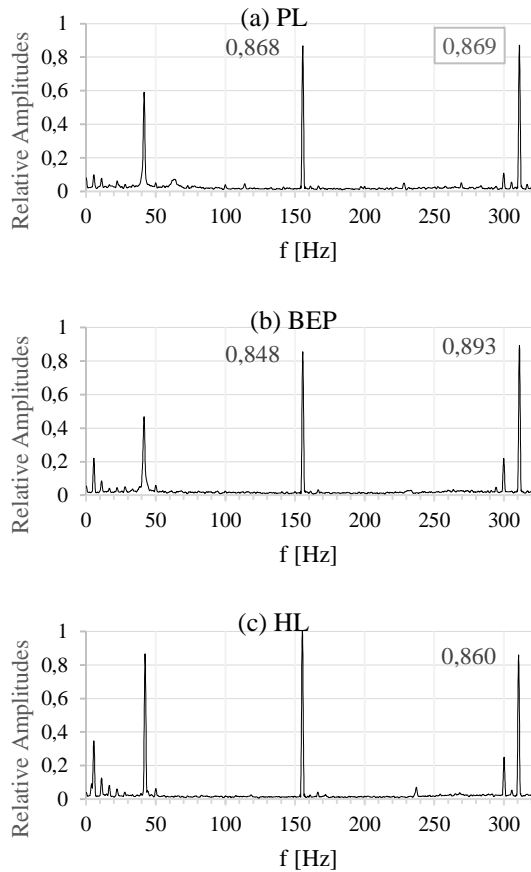


Figure 12 FFT of strain gauge signal. Amplitudes are normalized to highest common value.

To simplify the evaluation of the differential pressure over the runner blade trailing edge, the RSI parts of PT14 was separated from the signal creating $PT14_{RSI}$ with the RSI part and $PT14^*$ as a signal without RSI. Then $PT14_{RSI}$ was shifted according to the phase shift on the inlet and added back with $PT14^*$ creating a signal $PT14_2$ as if it was measured on the opposite side of the blade. $PT14$ and $PT14_2$ was then subtracted, creating $\Delta PT14$. In Figure 13 the FFT of $PT14$ and $\Delta PT14$ is presented. It is clear that the guide vane frequency amplitude is reduced by 20%. The second harmonic is multiplied by a factor of 1,47. From equation (2) the theoretical amplification for RSI_g due to phase shift is calculated to 0,81 for first harmonic and 1,49 for second harmonic, thus theory and measurements coincide well.

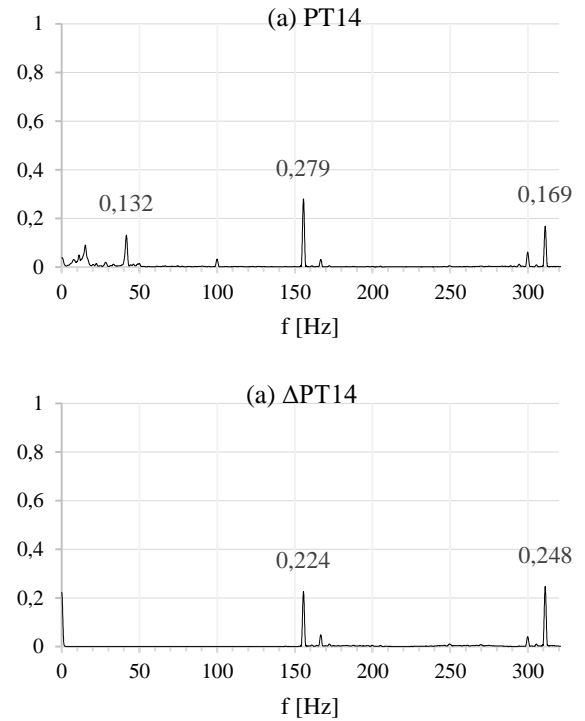


Figure 13 FFT of $PT14$ and $\Delta PT14$. Normalized as in Figure 9

IV. DISCUSSION

To find the amplitudes of the different components, a combination of Welch's method, inspection of raw signal and inspection of a filtered signal for the respective frequency did give equal results. It was not possible to give an exact value for the raw signal, but the filtered signal was used to calculate an average value and compared with FFT. The amplitudes are therefore considered reasonable.

Evaluation of the phase shift and the time delay between the signals was not possible by inspection, because the difference was smaller than the noise on the raw signal. This noise is also considered as an uncertainty when filtering, thus the phase shift

on a filtered signal is not considered trustworthy. For phase evaluation, the only method used was FFT, which should have an additional method for validation. However, the phase shift calculated by FFT between PT10 and PT11 proved to be within 0,4% of calculated value for RSI_g^1 as presented in Table 4. On the other hand, RSI_g^2 is not found to be within expected range. The RSI_g^2 is not fully understood, thus the FFT method for phase shift was used, despite the values calculated for RSI_g^2 .

The two sensors on the inlet of two different channels show coincident results, thus the measurements are considered representative for the actual pressure in the channel and is valuable for CFD validation.

By comparing the estimated speed of the pressure waves in the runner channel, the measurements indicates RSI_g^1 as a travelling wave along the splitter. The calculated speed in Table 5 is approximately the speed of sound inside the runner. With reflected waves, the measured speed will be below the speed of sound. The speed of sound should be evaluated in future measurements. Downstream the splitter, the RSI_g^1 is found with very low speed, even in reverse direction. With a perfect standing wave, the speed should be close to zero. Negative values indicates more reflected energy than incoming, which is unphysical. However, since the channel is not a straight smooth tube, the angle on the outlet may cause the reflections to travel up towards the hub and thus give the results presented. This is illustrated in **Figure 14**. Current setup is not able to determine if such phenomena exists. However, reflection at the outlet of the channel will be present since there is a sudden change in area to the draft tube, giving possible wave reflections.

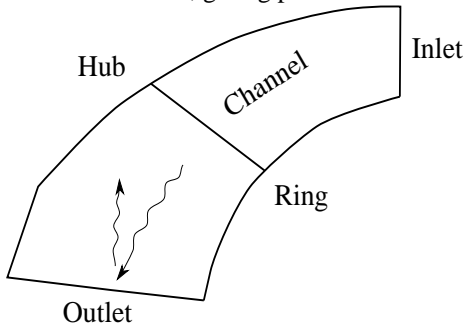


Figure 14 Possible reflection at the outlet.

The fact that the measurements indicate a travelling wave along splitter can be explained with the reduction of the amplitudes of RSI_g^1 as seen in **Figure 10**. If this reduction is equal for the reflected wave, it will dissipate before returning to the inlet and thus not give a standing wave. Another possibility is if the reflection coefficient is different for a wave travelling forward and backward in the same channel. For the forward travelling wave, the end of the splitter can appear as a smooth transition with reflection coefficient $R \sim 0$, while the reflected wave may experience this as a blockage or open ended tube with a higher absolute R . This is known as a trapped wave and illustrated in **Figure 15**. Future measurements without rotation of the runner and a single pulse triggered on the inlet could be

used to evaluate this phenomenon.

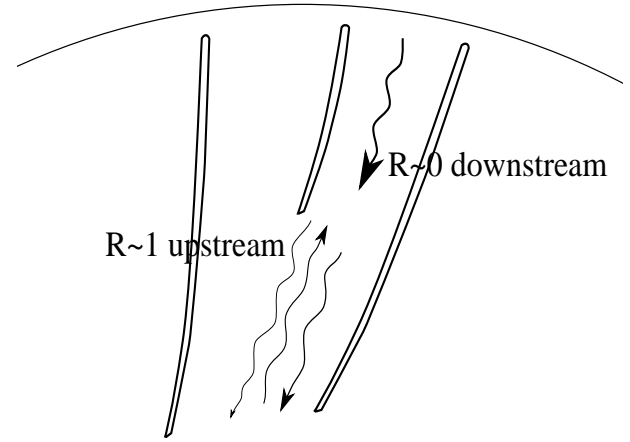


Figure 15 Trapped wave.

The high amplitude reduction of RSI_g^1 can be seen in relation to the curved channel and the mixing of two velocity fields past the splitter. In addition, the curved channel gives more reflections and more energy dissipation from the waves. Since there is a high pressure and low-pressure side of each blade and splitter, there will be a velocity field mixing downstream the splitter. This was explained by Kopro[8]. This mixing zone can be seen as a source for reducing the amplitudes of the pressure waves.

In **Figure 11** the RSI_g^2 amplitudes through the runner channel is presented. While the RSI_g^1 is reduced throughout the channel, the RSI_g^2 is higher at the middle of the channel and lower at the inlet and outlet. In addition, the calculated speed in Table 5 is indicating a wave travelling from the outlet to inlet of the runner for all running points. If the second harmonics is developing at the inlet of the runner together with the first harmonics, this development is not fully understood. The discussed reflection at the outlet is one possible explanation for higher amplitudes along the runner hub. Another possibility is the second pressure wave from the opposite side of the splitter joining at the trailing edge of the splitter. If these two waves join, the amplitude should increase at PT13. However, this does not explain the high amplitude at PT12, and is not consistent with the amplitudes related to RSI_g^1 . Higher amplitude of PT12 indicates that the reflected energy from both channels is returning in one channel. Measurements in both splitter channels could give more answers. However, this is not consistent with the trapped wave theory. A final consideration is that the second harmonic is initiated by vibration and not developed at the inlet of the runner channel. This could be more consistent with both the travelling speeds and the phase calculated. This needs further investigation.

The frequencies measured by the strain gauge are dominated by the RSI phenomena. As seen in **Figure 12**, the RSI_g^1 and the second harmonics is most dominating. When calculating the amplification created by the phase shifted pressure pulse in equation (2), it is quite evident that the higher harmonics are

amplified more than the first, thus care should be taken in the design phase evaluating higher harmonics and the risk of amplification.

V. CONCLUSION

The evaluation of the first harmonic of the guide vane passing frequency gave good results and was in correlation to earlier experiments. The measurement setup is considered to give valuable data for CFD verification. However, a full understanding of the pressure waves in the channel is not achieved with current analysis. On the other hand, if a CFD analysis is matching the measured pressure and strain, this could provide valuable information for explaining the physics in the runner channel. To get more information of the pressure waves inside the runner, further investigations with more sensors should be considered for both strain and pressure. The RSI frequency is found to be the most domination amplitude of the cyclic blade loading. The phase shift between two runner channels was used to validate the measurements and processing methods. The second harmonic of the RSI is not fully understood, both amplitudes and phase. However, the amplification due to phase shift was confirmed. Investigation of the measurements described in this paper, requires repetition. In addition, similar setup on different geometries could give valuable information for validation. The setup also provides the possibility to evaluate the propagating waves through the runner due to high frequency bandwidth.

VI. FURTHER WORK

To get a correct picture of the loading of the blades, more strain gauges will be mounted and if possible in rosette configuration for evaluation of the stress. In addition, blades that are more flexible and redesign of hub and shroud will be analyzed for truer scaling of the behavior of a prototype runner. Vibration modes should also be investigated as a possible cause for the higher harmonic amplitudes found. More pressure sensors will be considered for future measurements in this project.

ACKNOWLEDGMENT

The research was carried out as a part of High Head Francis research program sponsored by the Norwegian Research Council, The Norwegian Hydropower industry and the Norwegian Center for Hydropower. This support made this experiment possible.

VII. BIBLIOGRAPHY

- [1] C. G. Rodriguez, E. Egusquiza, X. Escaler, Q. W. Liang, and F. Avellan, "Experimental investigation of added mass effects on a Francis turbine runner in still water," *J. Fluids Struct.*, vol. 22, no. 5, pp. 699–712, Jul. 2006.
- [2] U. Seidel, B. Hübner, J. Löfflad, and P. Faigle, "Evaluation of RSI-induced stresses in Francis runners," *IOP Conf. Ser. Earth Environ. Sci.*, vol. 15, no. 5, p. 52010, 2012.
- [3] A. Coutu, R. Michel D, C. Monette, and B. Nennemann, "Experience with rotor-stator interactions in high head francis runner," *IAHR 24th Symp. Hydraul. Mach. Syst.*, Oct. 2008.
- [4] H. Brekke, "A Review on Oscillatory Problems in Francis Turbine," *New Trends Technol. Devices Comput. Commun. Ind. Syst. Sciyo*, pp. 217–232, 2010.
- [5] I. Oftebro and A. Lønning, "Paper 2: Pressure Oscillations in Francis Turbines," in *Proceedings of the Institution of Mechanical Engineers, Conference Proceedings*, 1966, vol. 181, pp. 119–124.
- [6] F. Duparchy, A. Favrel, P.-Y. Lowys, C. Landry, A. Müller, K. Yamamoto, and F. Avellan, "Analysis of the part load helical vortex rope of a Francis turbine using on-board sensors," *J. Phys. Conf. Ser.*, vol. 656, no. 1, p. 12061, 2015.
- [7] Pierre-Yves Lowys, Jean-Loup Deniau, Eric Gaudin, Pierre Leroy, and Mohand Djatout, "On-board model runner dynamic measurements," presented at the HydroVision, 2006.
- [8] E. Kobro, "Measurement of Pressure Pulsations in Francis Turbines (Doctoral Thesis)," NNTNU, EPT, 2010.
- [9] H. Bjørndal, R. André P, and H. Anders L., "Mechanical robustness of Francis runners, requirements to reduce the risk of cracks in blades," *Hydro 2011*, 2011.
- [10] H. Tanaka, "Vibration Behavior and Dynamic Stress of Runners of Very High Head Reversible Pump-turbines," *Int. J. Fluid Mach. Syst.*, vol. 4, no. 2, pp. 289–306, Jun. 2011.
- [11] Y. Kubota, T. Susuki, H. Tomita, T. Nagafugi, and C. Okamura, "Vibration of Rotating Bladed Disc Excited by Stationary Distributed Forces," *Bull. JSME*, vol. 26, no. 221, Nov. 1983.
- [12] C. G. Rodriguez, E. Egusquiza, and I. F. Santos, "Frequencies in the Vibration Induced by the Rotor Stator Interaction in a Centrifugal Pump Turbine," *J. Fluids Eng.*, vol. 129, no. 11, p. 1428, 2007.
- [13] E. B. Wylie and V. L. Streeter, *Fluid Transients*, 1st Edition. New York: McGraw-Hill Inc.,US, 1978.
- [14] "Francis-99 - NTNU." [Online]. Available: <http://www.ntnu.edu/nvks/francis-99>. [Accessed: 27-May-2016].
- [15] K. Kalita, N. Das, P. K. Boruah, and U. Sarma, "Design and Uncertainty Evaluation of a Strain Measurement System," *MAPAN*, vol. 31, no. 1, pp. 17–24, Mar. 2016.